

Dispersive approach to QCD and inclusive τ lepton hadronic decay

A.V. Nesterenko*

*Bogoliubov Laboratory of Theoretical Physics,
Joint Institute for Nuclear Research,
Dubna, 141980, Russian Federation*

Theoretical description of the inclusive τ lepton hadronic decay is performed in the framework of dispersive approach to QCD. The latter provides the unified integral representations for the hadronic vacuum polarization function, related R -function, and Adler function. These representations account for the intrinsically nonperturbative constraints, which originate in the kinematic restrictions on the functions on hand, and retain the effects due to hadronization, which play valuable role in the studies of the strong interaction processes at low energies. The dispersive approach proves to be capable of describing recently updated ALEPH and OPAL experimental data on inclusive τ lepton hadronic decay in vector and axial-vector channels. The vicinity of values of QCD scale parameter obtained in both channels testifies to the self-consistency of the developed approach.

PACS numbers: 11.55.Fv, 12.38.Aw, 12.38.Lg

I. INTRODUCTION

Hadronic vacuum polarization function $\Pi(q^2)$ plays a central role in various decisive tests of the self-consistency of Quantum Chromodynamics (QCD) and entire Standard Model, that, in turn, puts strong limits on possible New Physics beyond the latter. In particular, theoretical description of such processes as inclusive τ lepton hadronic decay, electron-positron annihilation into hadrons, as well as the hadronic contributions to the muon anomalous magnetic moment and to the running of the electromagnetic fine structure constant, is inherently based on $\Pi(q^2)$. Additionally, the theoretical analysis of these strong interaction processes constitutes a natural framework for a thorough study of both perturbative and intrinsically nonperturbative aspects of hadron dynamics.

The ultraviolet behavior of the hadronic vacuum polarization function can reliably be calculated by making use of perturbation theory. However, since the unambiguous method of description of the strong interaction processes at low energies is still far from being feasible, in order to shed some light on $\Pi(q^2)$ at low energies one inevitably resorts to a variety of nonperturbative approaches. For instance, some hints on the nonperturbative features of the hadronic vacuum polarization function can be gained from such methods as lattice simulation [1–3], operator product expansion [4–7], instanton liquid model [8, 9], and others.

* nesterav@theor.jinr.ru

One of the sources of the nonperturbative information about the low-energy hadron dynamics is provided by dispersion relations. Specifically, the latter render the physical kinematic restrictions¹ on the pertinent processes into the mathematical form. As a result, dispersion relations impose stringent constraints on relevant functions (such as $\Pi(q^2)$, related $R(s)$, and $D(Q^2)$, see Eqs. (1), (4), and (5) below), that should certainly be taken into account when one oversteps the limits of perturbation theory. These constraints are embodied within so-called dispersive approach to QCD, which furnishes unified integral representations for the functions on hand (see Sect. II).

The primary objective of this paper is to perform the analysis of inclusive τ lepton hadronic decay in the framework of dispersive approach to QCD, that, in particular, would allow to properly account for the effects due to nonvanishing hadronic production threshold.

The layout of the paper is as follows. In Section II the general dispersion relations for the hadronic vacuum polarization function, so-called R -function, and Adler function are discussed (subsection II A) and dispersive approach to QCD is overviewed (subsection II B). Section III deals with the inclusive τ lepton hadronic decay. Specifically, subsection III A contains general remarks on this strong interaction process, whereas its theoretical description is briefly recounted in subsection III B. The analysis of recently updated ALEPH [10, 11] and OPAL [12, 13] experimental data on inclusive τ lepton hadronic decay within perturbative and dispersive approaches is performed in subsections III C and III D, respectively. In Conclusions (Sect. IV) the basic results are summarized and further studies within this approach are outlined.

II. DISPERSIVE APPROACH TO QUANTUM CHROMODYNAMICS

A. General dispersion relations for $\Pi(q^2)$, $R(s)$, and $D(Q^2)$

As mentioned in the Introduction, theoretical description of a number of the strong interaction processes is inherently based on the hadronic vacuum polarization function $\Pi(q^2)$. The latter is defined as the scalar part of the hadronic vacuum polarization tensor

$$\begin{aligned}\Pi_{\mu\nu}(q^2) &= i \int d^4x e^{iqx} \langle 0 | T \{ J_\mu(x) J_\nu(0) \} | 0 \rangle \\ &= \frac{i}{12\pi^2} (q_\mu q_\nu - g_{\mu\nu} q^2) \Pi(q^2).\end{aligned}\tag{1}$$

For the processes involving final state hadrons the function $\Pi(q^2)$ (1) has the only cut along the positive semiaxis of real q^2 starting at the nonvanishing hadronic production threshold $q^2 \geq m^2$ (see discussion of this issue in, e.g., book [14]). In particular, the Feynman amplitude of the respective process vanishes for the energies below the threshold, that expresses the physical fact that the production of the final state hadrons is kinematically forbidden for $q^2 < m^2$ (see also papers [15–17] and references therein). Once the location of cut of function $\Pi(q^2)$ in the complex q^2 -plane is known, one can write down the corresponding dispersion relation. Specifically, bearing in mind the asymptotic ultraviolet behavior of

¹ For example, the fact that the hadronic production threshold has a nonvanishing value.

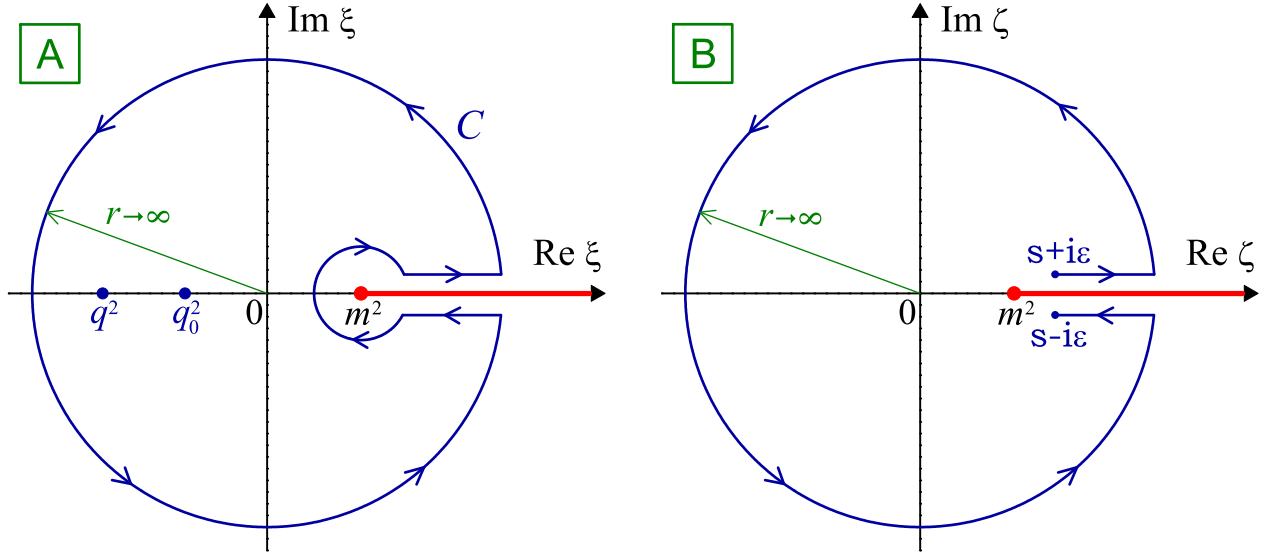


FIG. 1. Left panel (A): The closed integration contour C in Eq. (2). The physical cut $\xi \geq m^2$ of the hadronic vacuum polarization function $\Pi(\xi)$ (1) is shown along the positive semiaxis of real ξ . Right panel (B): The integration contour in Eq. (7). The physical cut $\zeta \geq m^2$ of the Adler function $D(-\zeta)$ (5) is shown along the positive semiaxis of real ζ .

the hadronic vacuum polarization function, it is convenient to employ the once-subtracted Cauchy integral formula:

$$\Delta\Pi(q^2, q_0^2) = \frac{1}{2\pi i} (q^2 - q_0^2) \oint_C \frac{\Pi(\xi)}{(\xi - q^2)(\xi - q_0^2)} d\xi. \quad (2)$$

In this equation $\Delta\Pi(q^2, q_0^2) = \Pi(q^2) - \Pi(q_0^2)$, whereas the closed integration contour C , which encloses both points q^2 and q_0^2 (commonly, one chooses $q_0^2 = 0$) and goes counterclockwise along the circle of infinitely large radius, is displayed in Fig. 1 A. Equation (2) is usually represented in the following form (see, e.g., paper [18]):

$$\Delta\Pi(q^2, q_0^2) = (q^2 - q_0^2) \int_{m^2}^{\infty} \frac{R(\sigma)}{(\sigma - q^2)(\sigma - q_0^2)} d\sigma, \quad (3)$$

where $R(s)$ stands for the discontinuity of the hadronic vacuum polarization function across the physical cut

$$\begin{aligned} R(s) &= \frac{1}{2\pi i} \lim_{\varepsilon \rightarrow 0_+} [\Pi(s + i\varepsilon) - \Pi(s - i\varepsilon)] \\ &= \frac{1}{\pi} \text{Im} \lim_{\varepsilon \rightarrow 0_+} \Pi(s + i\varepsilon), \end{aligned} \quad (4)$$

which is identified with the so-called R -ratio of electron-positron annihilation into hadrons. It is worthwhile to note that in Eq. (4) the second equality holds for the functions $\Pi(q^2)$ satisfying the condition $\Pi(\xi^*) = \Pi^*(\xi)$ only.

For practical purposes, it is convenient to define the Adler function [19]

$$D(Q^2) = -\frac{d\Pi(-Q^2)}{d\ln Q^2}, \quad (5)$$

with $Q^2 = -q^2 = -s > 0$ being the spacelike kinematic variable. It is worth mentioning that the subtraction point q_0^2 , appearing in Eq. (3), does not enter in Eqs. (4) and (5). The dispersion relation for the Adler function $D(Q^2)$ follows directly from Eqs. (3) and (5), namely [19]

$$D(Q^2) = Q^2 \int_{m^2}^{\infty} \frac{R(\sigma)}{(\sigma + Q^2)^2} d\sigma. \quad (6)$$

In turn, the inverse relations, which express the functions (1) and (4) in terms of the Adler function, can be obtained by integrating Eq. (5) in finite limits, specifically

$$R(s) = \frac{1}{2\pi i} \lim_{\varepsilon \rightarrow 0+} \int_{s+i\varepsilon}^{s-i\varepsilon} D(-\zeta) \frac{d\zeta}{\zeta}, \quad (7)$$

see Refs. [20, 21], and

$$\Delta\Pi(-Q^2, -Q_0^2) = - \int_{Q_0^2}^{Q^2} D(\zeta) \frac{d\zeta}{\zeta}, \quad (8)$$

see Ref. [22]. The integration contour in Eq. (7) lies in the region of analyticity of the integrand, see Fig. 1 B.

It is worthwhile to outline that the derivation of relations (3), (6)–(8) requires only the knowledge of the location of cut of hadronic vacuum polarization function $\Pi(q^2)$ (1) in the complex q^2 -plane, the asymptotic ultraviolet behavior of $\Pi(q^2)$, and the definitions (4) and (5). The derivation of relations (3), (6)–(8) involves neither additional approximations nor phenomenological assumptions.

As noted above, the aforementioned kinematic restrictions on the process on hand are inherently embodied within corresponding dispersion relations. In turn, the latter impose stringent physical intrinsically nonperturbative constraints on the functions $\Pi(q^2)$, $R(s)$, and $D(Q^2)$, that should certainly be accounted for when one comes out of the limits of perturbation theory. For example, Eq. (3) implies that the hadronic vacuum polarization function $\Pi(q^2)$ has the only cut along the positive semiaxis of real q^2 starting at the hadronic production threshold $q^2 \geq m^2$, whereas Eqs. (4) and (7) signify that the function $R(s)$ acquires non-zero values for real s above the threshold ($s \geq m^2$) only and accounts for the effects² due to continuation of spacelike theoretical results into timelike domain. In turn, Eq. (6) implies that the Adler function vanishes³ in the infrared limit ($D(Q^2) \rightarrow 0$ at $Q^2 \rightarrow 0$) and possesses the only cut along the negative semiaxis of real Q^2 starting at the hadronic production threshold $Q^2 \leq -m^2$ (see papers [16, 22, 28] and references therein).

B. Novel integral representations for $\Pi(q^2)$, $R(s)$, and $D(Q^2)$

Equations (3)–(8) constitute the complete set of relations, which express the functions $\Pi(q^2)$, $R(s)$, and $D(Q^2)$ in terms of each other. For practical purposes, it proves to be convenient to deal with the unified integral representations, which express the functions on hand in terms of the common spectral density $\rho(\sigma)$. Such representations are obtained in

² Such as the so-called “ π^2 -terms”, see, e.g., papers [23–25], Sect. 2.5 of review [26], as well as Ref. [27].

³ This condition holds for $m^2 \neq 0$ only.

the framework of the so-called dispersive approach to QCD (see papers [15, 16, 22, 28] and references therein).

In particular, the integral representation for the function $R(s)$ (4) can be derived from Eq. (7) (the proper integration contour is displayed in Fig. 1 B) and the fact that the strong correction to the Adler function vanishes in the ultraviolet asymptotic:

$$R(s) = R^{(0)}(s) + \theta(s - m^2) \int_s^\infty \rho(\sigma) \frac{d\sigma}{\sigma}. \quad (9)$$

In this equation $R^{(0)}(s)$ denotes the leading-order (i.e., zeroth order in the strong running coupling) term of the function $R(s)$, $\theta(x)$ is the unit step-function ($\theta(x) = 1$ if $x \geq 0$ and $\theta(x) = 0$ otherwise), and $\rho(\sigma)$ stands for the spectral density specified in Eq. (12) below. In turn, integral representation for the hadronic vacuum polarization function (1) can be obtained⁴ by making use of Eqs. (3) and (9)

$$\begin{aligned} \Delta\Pi(q^2, q_0^2) &= \Delta\Pi^{(0)}(q^2, q_0^2) \\ &+ \int_{m^2}^\infty \rho(\sigma) \ln\left(\frac{\sigma - q^2}{\sigma - q_0^2} \frac{m^2 - q_0^2}{m^2 - q^2}\right) \frac{d\sigma}{\sigma}, \end{aligned} \quad (10)$$

whereas integral representation for the Adler function (5) can be derived directly from Eqs. (5) and (10)

$$D(Q^2) = D^{(0)}(Q^2) + \frac{Q^2}{Q^2 + m^2} \int_{m^2}^\infty \rho(\sigma) \frac{\sigma - m^2}{\sigma + Q^2} \frac{d\sigma}{\sigma}. \quad (11)$$

The spectral density appearing in Eqs. (9)–(11) reads

$$\begin{aligned} \rho(\sigma) &= \frac{1}{2\pi i} \frac{d}{d \ln \sigma} \lim_{\varepsilon \rightarrow 0_+} \left[p(\sigma - i\varepsilon) - p(\sigma + i\varepsilon) \right] \\ &= -\frac{d}{d \ln \sigma} r(\sigma) \\ &= \frac{1}{2\pi i} \lim_{\varepsilon \rightarrow 0_+} \left[d(-\sigma - i\varepsilon) - d(-\sigma + i\varepsilon) \right]. \end{aligned} \quad (12)$$

Here $p(q^2)$, $r(s)$, and $d(Q^2)$ denote the strong corrections to the functions $\Pi(q^2)$, $R(s)$, and $D(Q^2)$, respectively. For the functions $p(q^2)$ and $d(Q^2)$ satisfying conditions $p(\xi^*) = p^*(\xi)$ and $d(\xi^*) = d^*(\xi)$ Eq. (12) acquires the form

$$\begin{aligned} \rho(\sigma) &= \frac{1}{\pi} \frac{d}{d \ln \sigma} \operatorname{Im} \lim_{\varepsilon \rightarrow 0_+} p(\sigma - i\varepsilon) \\ &= -\frac{d}{d \ln \sigma} r(\sigma) \\ &= \frac{1}{\pi} \operatorname{Im} \lim_{\varepsilon \rightarrow 0_+} d(-\sigma - i\varepsilon). \end{aligned} \quad (13)$$

It is straightforward to verify that the functions (9)–(11) satisfy all the relations (3)–(8). In particular, the latter means that the representation (9) can also be obtained from Eqs. (4)

⁴ Derivation of Eq. (10) from Eqs. (3) and (9) involves the integration by parts.

and (10), the representation (11) can also be derived from Eqs. (6) and (9), etc. The discussion of this issue can be found in papers [16, 17, 22, 28–30] and references therein.

The leading-order terms in Eqs. (9)–(11) have the following form [14, 33]:

$$\begin{aligned}\Delta\Pi^{(0)}(q^2, q_0^2) &= \frac{2}{\tan^3\varphi}(\varphi - \tan\varphi) \\ &\quad - \frac{2}{\tan^3\varphi_0}(\varphi_0 - \tan\varphi_0),\end{aligned}\tag{14a}$$

$$R^{(0)}(s) = \theta(s - m^2) \left(1 - \frac{m^2}{s}\right)^{3/2},\tag{14b}$$

$$D^{(0)}(Q^2) = 1 + \frac{3}{\xi} \left[1 - \sqrt{1 + \xi^{-1}} \sinh^{-1}(\xi^{1/2})\right],\tag{14c}$$

where $\sin^2\varphi = q^2/m^2$, $\sin^2\varphi_0 = q_0^2/m^2$, and $\xi = Q^2/m^2$, see also Refs. [22, 29, 30]. It is worth mentioning here that a rough approximation for the leading-order terms of the functions (9)–(11) (the so-called “Abrupt kinematic threshold”)

$$\Delta\Pi_{\text{AKT}}^{(0)}(q^2, q_0^2) = -\ln\left(\frac{m^2 - q^2}{m^2 - q_0^2}\right),\tag{15a}$$

$$D_{\text{AKT}}^{(0)}(Q^2) = \frac{Q^2}{Q^2 + m^2},\tag{15b}$$

$$R_{\text{AKT}}^{(0)}(s) = \theta(s - m^2),\tag{15c}$$

which, nonetheless, grasps the basic peculiarities of the functions on hand, was discussed in Refs. [16, 17, 22, 28, 29].

The integral representations (9)–(11) automatically embody all the nonperturbative constraints⁵, which Eqs. (3)–(8) impose on the functions on hand (see Sect. II A). It is worthwhile to note that a preliminary formulation of the dispersive approach to QCD, which accounts for only one of the aforementioned constraints on the Adler function (namely, the cut $Q^2 \leq -m^2$ along the negative semiaxis of real Q^2), was discussed in Refs. [15, 34]. The integral representations (9)–(11) were obtained by employing only the relations (3)–(8) and the asymptotic ultraviolet behavior of the hadronic vacuum polarization function. Neither additional approximations nor phenomenological assumptions were involved in the derivation of Eqs. (9)–(11). As one can infer from Fig. 2, the hadronic vacuum polarization function (10) is in a good agreement with relevant low-energy lattice simulation data [2], see Refs. [31, 32]. It is worth mentioning also that the Adler function (11) complies with corresponding experimental prediction in the entire energy range (see, in particular, Refs. [16, 17, 28]), and the representations (9)–(11) conform with the results obtained in Ref. [35].

So far, there is no method to restore the unique complete expression for the spectral density $\rho(\sigma)$ (12) (discussion of this issue may be found in, e.g., Refs. [22, 28, 36, 37]). Nonetheless, the perturbative contribution to $\rho(\sigma)$ can be calculated by making use of perturbative expression for either of the strong corrections appearing in Eq. (12) (see, e.g.,

⁵ Including the correct analytic properties in the kinematic variable, that implies that the functions (9)–(11) are free of unphysical singularities.

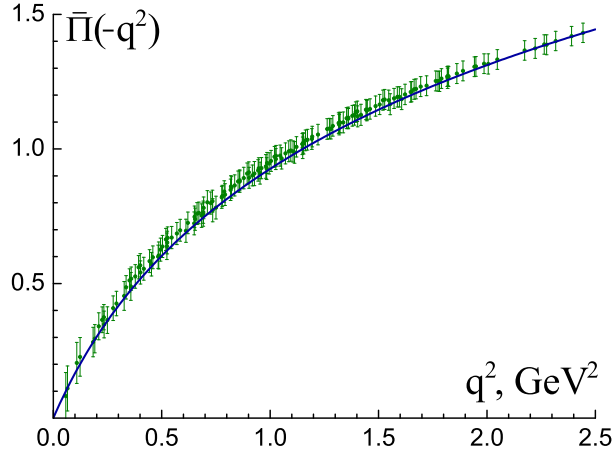


FIG. 2. Comparison of the hadronic vacuum polarization function (10) ($\bar{\Pi}(q^2) = \Delta\Pi(0, q^2)$, solid curve) with relevant lattice simulation data [2] (circles). The presented results correspond to the spectral density (17) and $n_f = 2$ active flavors, see Refs. [31, 32].

Ref. [38]):

$$\begin{aligned}
 \rho_{\text{pert}}(\sigma) &= \frac{1}{2\pi i} \frac{d}{d \ln \sigma} \lim_{\varepsilon \rightarrow 0_+} \left[p_{\text{pert}}(\sigma - i\varepsilon) - p_{\text{pert}}(\sigma + i\varepsilon) \right] \\
 &= -\frac{d}{d \ln \sigma} r_{\text{pert}}(\sigma) \\
 &= \frac{1}{2\pi i} \lim_{\varepsilon \rightarrow 0_+} \left[d_{\text{pert}}(-\sigma - i\varepsilon) - d_{\text{pert}}(-\sigma + i\varepsilon) \right].
 \end{aligned} \tag{16}$$

In what follows the model [22, 29, 30] for the spectral density

$$\rho(\sigma) = \frac{4}{\beta_0} \frac{1}{\ln^2(\sigma/\Lambda^2) + \pi^2} + \frac{\Lambda^2}{\sigma} \tag{17}$$

will be adopted. The first term in the right-hand side of Eq. (17) is the one-loop perturbative contribution, whereas the second term represents intrinsically nonperturbative part of the spectral density (see also papers [36, 37]).

Note that in the massless limit ($m^2 = 0$) the integral representations (9)–(11) acquire the form

$$\begin{aligned}
 \Delta\Pi(q^2, q_0^2) &= \Delta\Pi_{\text{pert}}^{(0)}(q^2, q_0^2) \\
 &\quad + \int_0^\infty \rho(\sigma) \ln \left[\frac{1 - (\sigma/q^2)}{1 - (\sigma/q_0^2)} \right] \frac{d\sigma}{\sigma},
 \end{aligned} \tag{18a}$$

$$R(s) = \theta(s) \left[R_{\text{pert}}^{(0)}(s) + \int_s^\infty \rho(\sigma) \frac{d\sigma}{\sigma} \right], \tag{18b}$$

$$D(Q^2) = D_{\text{pert}}^{(0)}(Q^2) + \int_0^\infty \frac{\rho(\sigma)}{\sigma + Q^2} d\sigma, \tag{18c}$$

where the leading-order terms read

$$\Delta\Pi_{\text{pert}}^{(0)}(q^2, q_0^2) = -\ln\left(\frac{-q^2}{-q_0^2}\right), \quad (19a)$$

$$R_{\text{pert}}^{(0)}(s) = 1, \quad (19b)$$

$$D_{\text{pert}}^{(0)}(Q^2) = 1. \quad (19c)$$

It is worthwhile to mention that for the case of perturbative spectral density ($\rho(\sigma) = \text{Im } d_{\text{pert}}(-\sigma - i0_+)/\pi$) two massless equations (18b) and (18c) become identical to those of the so-called Analytic Perturbation Theory (APT) [39] (see also Refs. [40–45]).

However, it is essential to keep the value of the hadronic production threshold nonvanishing. Specifically, whereas in the ultraviolet asymptotic the effects due to hadronization (i.e., due to $m^2 \neq 0$) can be safely neglected, in the infrared domain such effects become substantial and play valuable role in the studies of the strong interaction processes at low energies. In particular, as it has been noted in subsection II A, the massless limit ($m^2 = 0$) loses some of the intrinsically nonperturbative constraints, which relevant dispersion relations impose on the functions on hand. For example, the difference between the representation (11) and its massless limit (18c) was elucidated in Sect. 4 of Ref. [16] and Sect. 3 of Ref. [17].

III. INCLUSIVE τ LEPTON HADRONIC DECAY

A. General remarks

The inclusive τ lepton hadronic decay is characterized by the experimentally measurable ratio of two widths:

$$R_\tau = \frac{\Gamma(\tau^- \rightarrow \text{hadrons}^- \nu_\tau)}{\Gamma(\tau^- \rightarrow e^- \bar{\nu}_e \nu_\tau)}. \quad (20)$$

This inclusive semileptonic branching ratio is usually decomposed into several parts, specifically

$$R_\tau = R_{\tau,V}^{J=0} + R_{\tau,V}^{J=1} + R_{\tau,A}^{J=0} + R_{\tau,A}^{J=1} + R_{\tau,S}. \quad (21)$$

In the right-hand side of this equation the first four terms account for the hadronic decay modes involving light quarks (u, d) only and associated with vector (V) and axial-vector (A) quark currents, respectively. The last term in the right-hand side of Eq. (21) accounts for the τ lepton hadronic decay modes which involve strange quark. The superscript J in Eq. (21) indicates the angular momentum in the hadronic rest frame.

Basically, the evaluation of the quantities appearing in Eq. (21) involves the so-called spectral functions, which are extracted from the experiment. For the zero angular momentum ($J = 0$) the vector spectral function vanishes (that yields $R_{\tau,V}^{J=0} = 0$), whereas the axial-vector one is commonly approximated by Dirac δ -function, since the main contribution is due to the pion pole here. The experimental predictions for the nonstrange spectral functions corresponding to $J = 1$ by ALEPH [10, 11] and OPAL [12, 13] Collaborations are

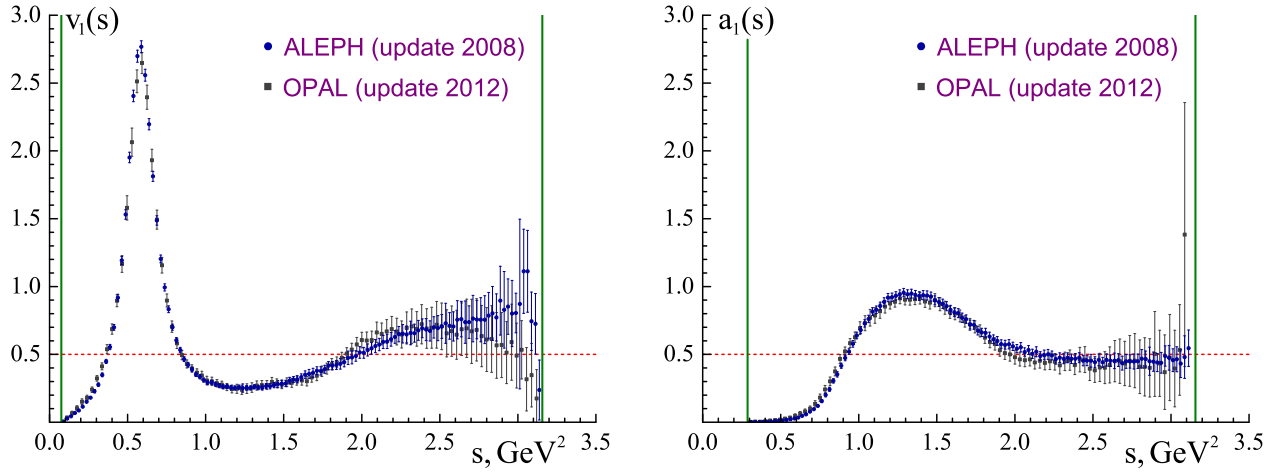


FIG. 3. The inclusive τ lepton hadronic decay vector (left-hand plot) and axial-vector (right-hand plot) spectral functions. The experimental data [11] (update of the ALEPH measurement [10]) and [13] (update of the OPAL measurement [12]) are shown by circles and boxes, respectively. Vertical solid lines mark the boundaries of respective kinematic intervals, whereas horizontal dashed line denotes the naive massless parton model prediction.

displayed in Fig. 3. In what follows we shall restrict ourselves to the study of the terms $R_{\tau,V}^{J=1}$ and $R_{\tau,A}^{J=1}$ of R_τ -ratio (21).

The theoretical expression for the aforementioned quantities reads

$$R_{\tau,V/A}^{J=1} = \frac{N_c}{2} |V_{ud}|^2 S_{EW} \left(\Delta_{QCD}^{V/A} + \delta'_{EW} \right), \quad (22)$$

where $N_c = 3$ is the number of colors, $|V_{ud}| = 0.97425 \pm 0.00022$ is Cabibbo–Kobayashi–Maskawa matrix element [46], $S_{EW} = 1.0194 \pm 0.0050$ and $\delta'_{EW} = 0.0010$ stand for the electroweak corrections [47], and

$$\Delta_{QCD}^{V/A} = 2 \int_{m_{V/A}^2}^{M_l^2} \left(1 - \frac{s}{M_l^2} \right)^2 \left(1 + 2 \frac{s}{M_l^2} \right) R(s) \frac{ds}{M_l^2} \quad (23)$$

denotes the hadronic contribution, see Ref. [48]. The function $R(s)$ appearing in the integrand of Eq. (23) is defined in Eq. (4). The experimental predictions for the functions $\Delta_{QCD}^{V/A}$ (23) corresponding to the recently updated ALEPH [11] and OPAL [13] data are, respectively,

$$\Delta_{exp}^V = 1.224 \pm 0.050, \quad \Delta_{exp}^A = 0.748 \pm 0.034, \quad (24a)$$

$$\Delta_{exp}^V = 1.229 \pm 0.088, \quad \Delta_{exp}^A = 0.741 \pm 0.058. \quad (24b)$$

It is worthwhile to note that in Eq. (23) M_l denotes the mass of the lepton on hand, whereas $m_{V/A}$ stands for the value of the hadronic production threshold (i.e., the total mass of the lightest allowed hadronic decay mode of this lepton in the corresponding channel). The nonvanishing value of $m_{V/A}$, which exceeds the masses of two lightest leptons, explicitly expresses the physical fact that τ lepton is the only lepton which is heavy enough

($M_\tau \simeq 1.777 \text{ GeV}$ [46]) to decay into hadrons. Specifically, in the massless limit ($m_{V/A} = 0$) the theoretical prediction (31) for the hadronic contribution (23) to Eq. (22) is nonvanishing for either lepton ($l = e, \mu, \tau$). In particular, the leading-order term of Eq. (31) ($\Delta_{\text{pert}}^{(0)} = 1$), which corresponds to the naive massless parton model prediction (19), does not depend on M_l , and, therefore, is the same for any lepton. In the realistic case (i.e., when the total mass of the lightest allowed hadronic decay mode exceeds the masses of electron and muon, $M_e < M_\mu < m_{V/A} < M_\tau$) Eq. (23) acquires non-zero value for the case of the τ lepton only (discussion of this issue can also be found in papers [22, 30] and references therein).

B. Theoretical evaluation of $\Delta_{\text{QCD}}^{V/A}$

Theoretical analysis of the hadronic contribution (23) to Eq. (22) usually begins with the integration by parts, that casts Eq. (23) into the form⁶ (the indices “V” and “A” will only be shown when relevant hereinafter)

$$\Delta_{\text{QCD}} = g(1)R(M_\tau^2) - g(\chi)R(m^2) + \frac{1}{2\pi i} \int_{C_1+C_2} g\left(\frac{\zeta}{M_\tau^2}\right) D(-\zeta) \frac{d\zeta}{\zeta}. \quad (25)$$

Here the functions $R(s)$ and $D(Q^2)$ are defined in Eqs. (4) and (5), respectively, $\chi = m^2/M_\tau^2$, and

$$g(x) = x(2 - 2x^2 + x^3). \quad (26)$$

The piecewise continuous integration contour appearing in the last term of Eq. (25) is displayed in Fig. 4 A. Specifically, the integration contour $C_1 + C_2$ consists of two straight lines, which go from $m^2 + i\varepsilon$ to $M_\tau^2 + i\varepsilon$ and from $M_\tau^2 - i\varepsilon$ to $m^2 - i\varepsilon$ (the limit $\varepsilon \rightarrow 0_+$ is assumed in what follows). If the Adler function $D(Q^2)$ appearing in the integrand of the last term of Eq. (25) possesses the correct analytic properties in the kinematic variable Q^2 (see Sect. II A), then the integration contour $C_1 + C_2$ can be continuously deformed into the integration contour $C_3 + C_4$ shown in Fig. 4 B:

$$\Delta_{\text{QCD}} = g(1)R(M_\tau^2) - g(\chi)R(m^2) + \frac{1}{2\pi i} \int_{C_3+C_4} g\left(\frac{\zeta}{M_\tau^2}\right) D(-\zeta) \frac{d\zeta}{\zeta}. \quad (27)$$

Here the integration contour C_3 is the non-closed circle of vanishing radius, which goes counterclockwise from $m^2 + i\varepsilon$ to $m^2 - i\varepsilon$, whereas the integration contour C_4 is the non-closed circle of radius M_τ^2 , which goes clockwise from $M_\tau^2 - i\varepsilon$ to $M_\tau^2 + i\varepsilon$.

Despite the remarks given in Sect. II, the massless limit ($m = 0$) will be adopted in the rest of this subsection and in the next subsection III C. Since the function $g(x)$ (26) vanishes at $x \rightarrow 0$, the second term in Eq. (27) and the integral along the contour C_3 (which

⁶ Derivation of Eq. (25) from Eq. (23) employs Eq. (7).

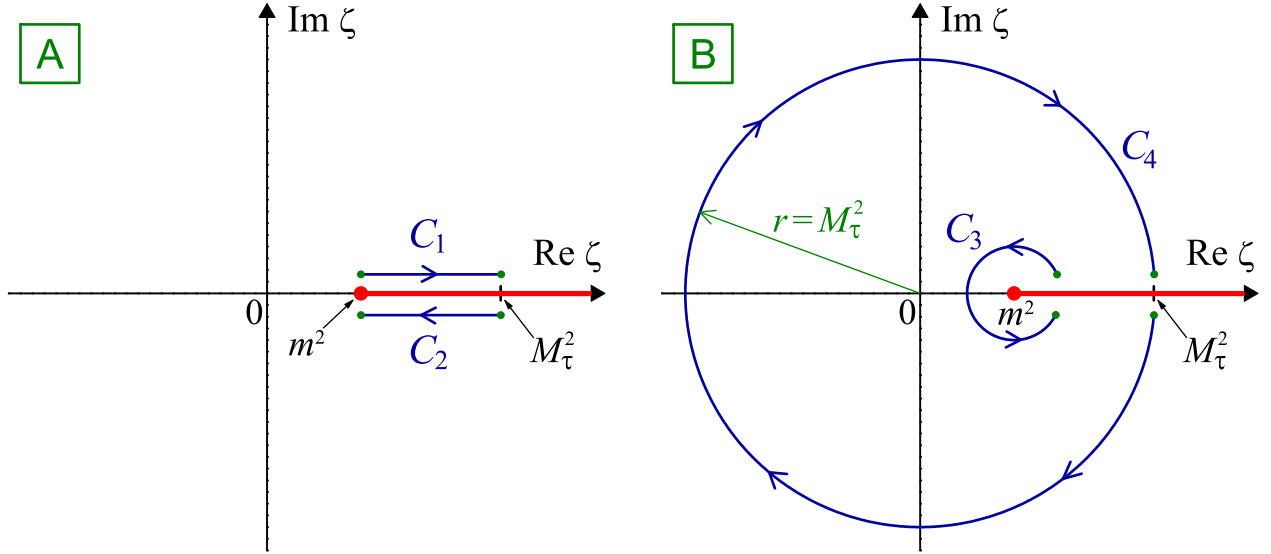


FIG. 4. The integration contour $C_1 + C_2$ in Eq. (25) (left-hand plot “A”) and its continuous deformation $C_3 + C_4$ (right-hand plot “B”). The physical cut $\zeta \geq m^2$ of the Adler function $D(-\zeta)$ (5) is shown along the positive semiaxis of real ζ .

is centered at $\zeta = 0$ in the massless limit) in the last term of Eq. (27) do not contribute⁷ to Δ_{QCD} , which takes the following form in this case:

$$\Delta_{\text{QCD}} = R(M_\tau^2) + \frac{1}{2\pi i} \int_{C_4} g\left(\frac{\zeta}{M_\tau^2}\right) D(-\zeta) \frac{d\zeta}{\zeta}. \quad (28)$$

The first term of this equation can be represented in the form of Eq. (7) with the integration contour C_4 shown in Fig. 4 B, that (after appropriate change of the integration variable) leads to

$$\Delta_{\text{QCD}} = \frac{1}{2\pi} \lim_{\varepsilon \rightarrow 0_+} \int_{-\pi+\varepsilon}^{\pi-\varepsilon} [1 - g(-e^{i\theta})] D(M_\tau^2 e^{i\theta}) d\theta. \quad (29)$$

C. Inclusive τ lepton hadronic decay within perturbative approach

From the very beginning, it is necessary to outline that the obtained in previous subsection Eq. (29) is only valid for the massless limit of the Adler function $D(Q^2)$, which possesses the correct⁸ analytic properties in the kinematic variable Q^2 . However, in the framework of perturbative approach one commonly directly employs in Eq. (29) the perturbative approximation $D_{\text{pert}}(Q^2)$, which has unphysical singularities in Q^2 . Specifically, at the ℓ -loop level

$$D_{\text{pert}}^{(\ell)}(Q^2) = D_{\text{pert}}^{(0)}(Q^2) + \sum_{j=1}^{\ell} d_j \left[\alpha_{\text{pert}}^{(\ell)}(Q^2) \right]^j. \quad (30)$$

⁷ The regular behavior of functions $R(s)$ and $D(Q^2)$ at the threshold is assumed here.

⁸ Otherwise, Eq. (29) can not be derived from Eq. (23).

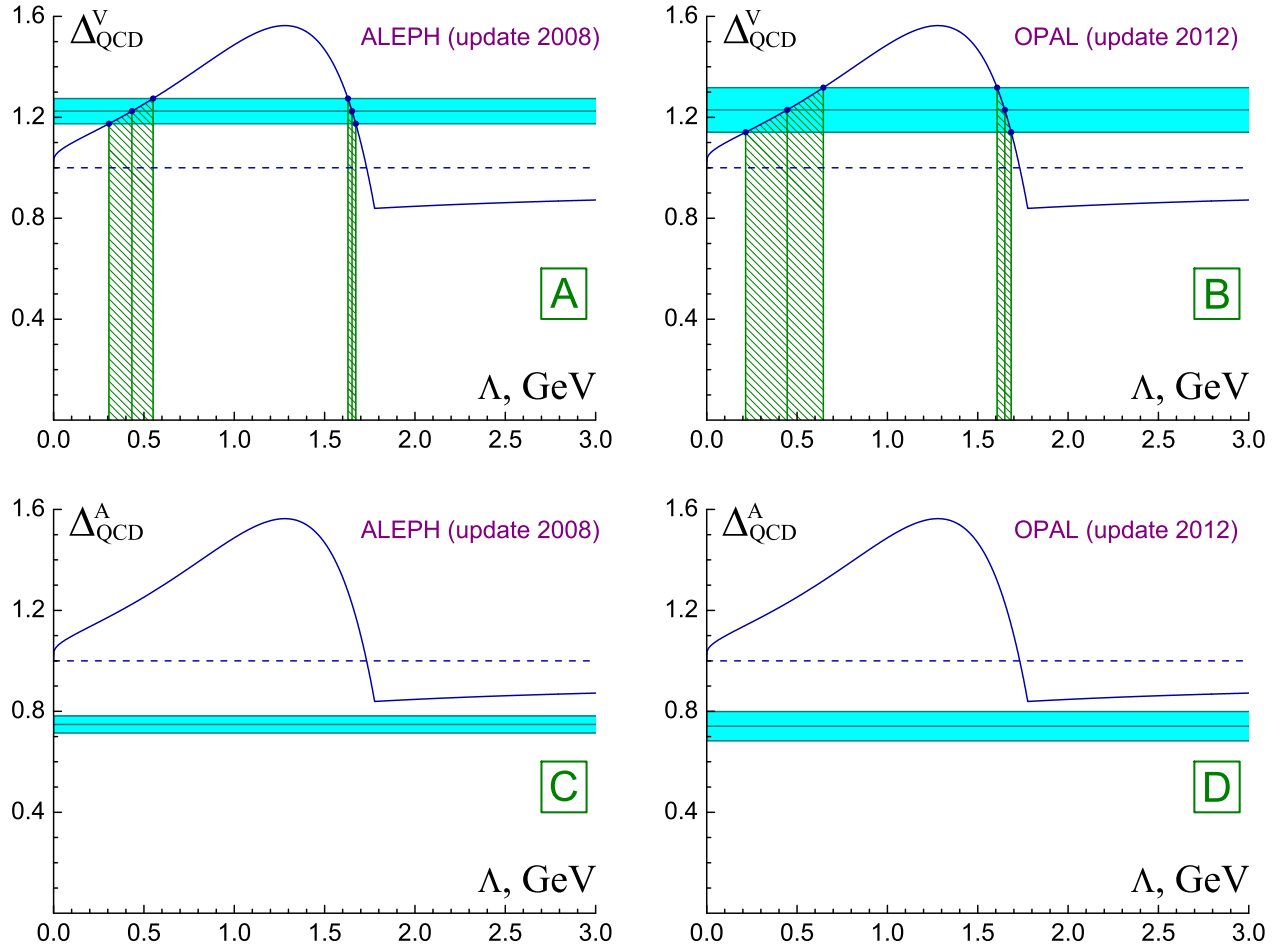


FIG. 5. Comparison of the perturbative expression $\Delta_{\text{pert}}^{V/A}$ (31) (solid curves) with relevant experimental data. The plots A, C and B, D correspond to Eq. (24a) (Ref. [11]) and Eq. (24b) (Ref. [13]), respectively. The leading-order term $\Delta_{\text{pert}}^{(0)}$ (31) is shown by horizontal dashed line, whereas the solution for QCD scale parameter Λ (if exists) is denoted by vertical dashed band.

In this equation at the one-loop level (i.e., for $\ell = 1$) the strong running coupling reads $\alpha_{\text{pert}}^{(1)}(Q^2) = 4\pi/[\beta_0 \ln(Q^2/\Lambda^2)]$, where $\beta_0 = 11 - 2n_f/3$, Λ denotes the QCD scale parameter, n_f stands for the number of active flavors, and $d_1 = 1/\pi$, see papers [49, 50] and references therein. In what follows the one-loop level with $n_f = 3$ active flavors will be assumed.

Thus, the substitution of the one-loop perturbative expression for the Adler function (30) to Eq. (29) eventually leads to

$$\Delta_{\text{pert}}^{V/A} = \Delta_{\text{pert}}^{(0)} + \frac{4}{\beta_0} \int_0^\pi \frac{\lambda A_1(\theta) + \theta A_2(\theta)}{\pi(\lambda^2 + \theta^2)} d\theta. \quad (31)$$

In this equation $\Delta_{\text{pert}}^{(0)} = 1$, $\lambda = \ln(M_\tau^2/\Lambda^2)$, and

$$A_1(\theta) = 1 + 2\cos(\theta) - 2\cos(3\theta) - \cos(4\theta), \quad (32)$$

$$A_2(\theta) = 2\sin(\theta) - 2\sin(3\theta) - \sin(4\theta). \quad (33)$$

Note that the leading-order term in the right-hand side of Eq. (31) ($\Delta_{\text{pert}}^{(0)} = 1$) corresponds to a rather rough massless perturbative approximation of the functions on hand (19), which is

TABLE I. Values of the QCD scale parameter Λ [MeV] obtained within perturbative approach (see Eq. (31) and Fig. 5).

| | ALEPH data (Eq. (24a), Ref. [11]) | | OPAL data (Eq. (24b), Ref. [13]) | |
|----------------------|---------------------------------------|--------------------|---------------------------------------|--------------------|
| vector channel | <u>434^{+117}_{-127}</u> | 1652^{+21}_{-23} | <u>445^{+201}_{-230}</u> | 1650^{+36}_{-43} |
| axial-vector channel | — | | — | |

applicable, in fact, in the ultraviolet asymptotic only. Besides, this leading-order term $\Delta_{\text{pert}}^{(0)}$ appears to be independent of any of the involved kinematic parameters (see also discussion of this issue in subsection III A and Refs. [22, 30]).

It is worth emphasizing that perturbative approach provides identical expressions (31) for the functions (23) in vector and axial-vector channels (i.e., $\Delta_{\text{pert}}^{\text{V}} \equiv \Delta_{\text{pert}}^{\text{A}}$). However, their experimental values [10–13] specified in Eq. (24) are different (i.e., $\Delta_{\text{exp}}^{\text{V}} \neq \Delta_{\text{exp}}^{\text{A}}$). The juxtaposition of the perturbative expression (31) with its experimental predictions (24) is presented in Fig. 5 and the obtained results are listed in Tab. I. As one can infer from Fig. 5 (plots A and B), for vector channel there are two⁹ solutions for the QCD scale parameter Λ . As for the axial-vector channel, the experimental data [10–13] can not be described within perturbative approach. In particular, the use of the massless limit results in the fact that the leading-order term of Eq. (31) far exceeds the corresponding experimental prediction $\Delta_{\text{exp}}^{\text{A}}$. Specifically, as one can infer from Fig. 5 (plots C and D), for any value of the QCD scale parameter Λ the function $\Delta_{\text{pert}}^{\text{A}}$ (31) lies above $\Delta_{\text{exp}}^{\text{A}}$ specified in Eq. (24).

D. Inclusive τ lepton hadronic decay within dispersive approach

It is crucial to emphasize that the effects due to the nonvanishing value of the hadronic production threshold have been completely left out in the massless limit¹⁰ examined above. However, as it was outlined in Sect. II, such effects play significant role in the studies of the strong interaction processes at low energies. The dispersive approach to QCD described in Sect. II properly accounts for the effects due to hadronization and embodies the aforementioned intrinsically nonperturbative constraints on the functions on hand. In the analysis of the inclusive τ lepton hadronic decay presented in this subsection¹¹ the integral representations obtained within dispersive approach to QCD (9)–(11) will be employed and the hadronic production threshold will be kept nonvanishing.

As noted above, the functions (9)–(11) possess the correct analytic properties in the kinematic variable. Hence, their use with any equivalent transformation of the initial expression (23) of the hadronic contribution $\Delta_{\text{QCD}}^{\text{V/A}}$ to Eq. (22) leads to the same result. For instance, one can use the representation (9) in Eq. (23), as well as the representations (9)

⁹ Usually, for vector channel the underlined value of Λ given in Tab. I is retained, whereas the other value is considered as formal solution and merely disregarded.

¹⁰ It is worthwhile to mention that there is a number of papers, which study the inclusive semileptonic branching ratio (21) within massless APT and its modifications, see Refs. [51, 52]. However, these papers basically deal either with the total sum of vector and axial-vector terms of Eq. (21) or with the vector term of Eq. (21) only.

¹¹ Description of the inclusive τ lepton hadronic decay given in Ref. [15] corresponds to the preliminary formulation of dispersive approach to QCD, which does not account for some of nonperturbative constraints on the functions on hand, see Sect. II.

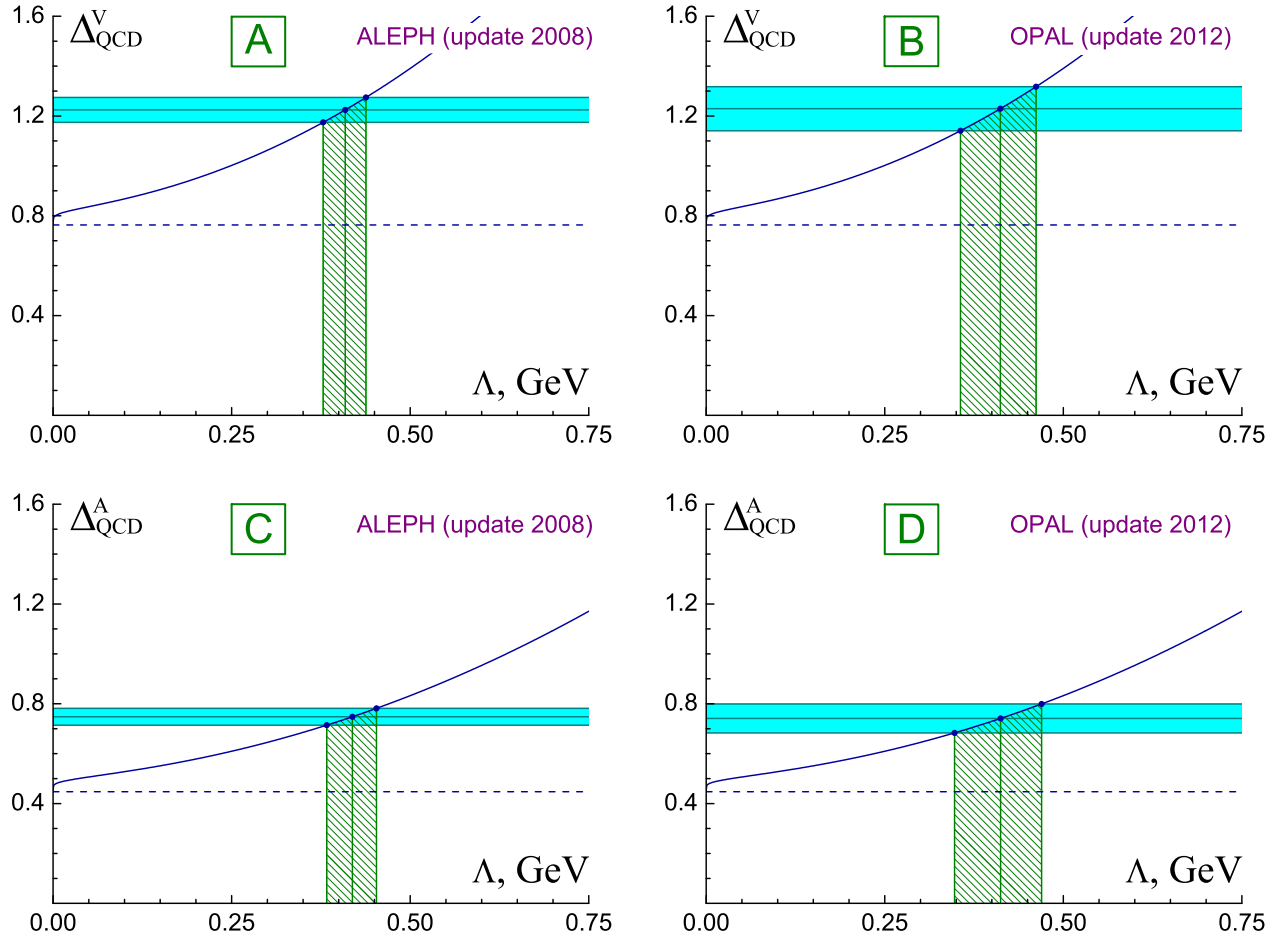


FIG. 6. Comparison of the expression $\Delta_{\text{QCD}}^{V/A}$ (34) (solid curves) with relevant experimental data. The plots A, C and B, D correspond to Eq. (24a) (Ref. [11]) and Eq. (24b) (Ref. [13]), respectively. The leading-order term (34) is shown by horizontal dashed line, whereas the solution for QCD scale parameter Λ is denoted by vertical dashed band.

and (11) in Eq. (27). Eventually, in the framework of the dispersive approach to QCD the hadronic contribution (23) to Eq. (22) acquires the following form

$$\begin{aligned} \Delta_{\text{QCD}}^{V/A} = & 3g_1\left(\frac{\chi_{V/A}}{2}\right)\sqrt{1-\chi_{V/A}} \\ & - 3g_2\left(\frac{\chi_{V/A}}{4}\right)\ln\left(\sqrt{\chi_{V/A}^{-1}} + \sqrt{\chi_{V/A}^{-1}-1}\right) \\ & + \int_{m_{V/A}^2}^{\infty} G\left(\frac{\sigma}{M_\tau^2}\right)\rho(\sigma)\frac{d\sigma}{\sigma}, \end{aligned} \quad (34)$$

where $\chi_{V/A} = m_{V/A}^2/M_\tau^2$, $m_V^2 \simeq 0.075 \text{ GeV}^2$, $m_A^2 \simeq 0.288 \text{ GeV}^2$, $G(x) = g(x)\theta(1-x) + g(1)\theta(x-1) - g(\chi_{V/A})$, spectral density $\rho(\sigma)$ is specified in Eq. (17), function $g(x)$ is defined in Eq. (26), and

$$g_1(x) = \frac{1}{3} + 4x - \frac{5}{6}x^2 + \frac{1}{2}x^3, \quad (35)$$

$$g_2(x) = 8x(1 + 2x^2 - 2x^3), \quad (36)$$

TABLE II. Values of the QCD scale parameter Λ [MeV] obtained within dispersive approach (see Eq. (34) and Fig. 6).

| | ALEPH data (Eq. (24a), Ref. [11]) | OPAL data (Eq. (24b), Ref. [13]) |
|----------------------|-----------------------------------|----------------------------------|
| vector channel | 408 ± 30 | 409 ± 53 |
| axial-vector channel | 418 ± 35 | 409 ± 61 |

see also papers [22, 29, 30] and references therein.

The juxtaposition of the obtained result (34) with pertinent experimental predictions (24) is presented in Fig. 6 and the corresponding values of QCD scale parameter Λ are given in Tab. II. As one can infer from Fig. 6, the dispersive approach is capable of describing the experimental data on inclusive τ lepton hadronic decay [10–13] in vector and axial-vector channels. The respective values of Λ conform to the one reported in the previous subsection. Additionally, the values of QCD scale parameter obtained in vector and axial-vector channels appear to be nearly identical to each other (see Tab. II), that testifies to the self-consistency of the developed approach.

IV. CONCLUSIONS

Theoretical description of inclusive τ lepton decay into hadrons is performed within dispersive approach to QCD. This approach enables one to retain the effects due to hadronization, which appear to be valuable in the low-energy domain, and to account for the intrinsically nonperturbative constraints, which originate in the kinematic restrictions on the process on hand. The obtained results indicate that the dispersive approach is capable of describing recently updated ALEPH [10, 11] and OPAL [12, 13] experimental data on inclusive τ lepton hadronic decay in vector and axial-vector channels. The values of QCD scale parameter Λ evaluated in both channels are nearly identical to each other, that bears witness to the self-consistency of the developed approach.

In further studies it would certainly be interesting to include into the presented analysis of inclusive τ lepton hadronic decay the higher order perturbative corrections as well as nonperturbative contributions arising from the operator product expansion.

ACKNOWLEDGMENTS

The author is grateful to D. Boito, P. Colangelo, M. Davier, F. De Fazio, S. Menke, and H. Wittig for the stimulating discussions and useful comments. The partial support of grant JINR-12-301-01 is acknowledged.

-
- [1] T. Blum, Phys. Rev. Lett. **91**, 052001 (2003); C. Aubin and T. Blum, Phys. Rev. D **75**, 114502 (2007); C. Aubin, T. Blum, M. Golterman, and S. Peris, *ibid.* **86**, 054509 (2012).

- [2] M. Della Morte, B. Jager, A. Juttner, and H. Wittig, AIP Conf. Proc. **1343**, 337 (2011); PoS (LATTICE 2011), 161 (2011); JHEP **1203**, 055 (2012).
- [3] M. Gockeler *et al.* [QCDSF Collaboration], Nucl. Phys. B **688**, 135 (2004); P. Boyle, L. Del Debbio, E. Kerrane, and J. Zanotti, Phys. Rev. D **85**, 074504 (2012).
- [4] M.A. Shifman, A.I. Vainshtein, and V.I. Zakharov, Nucl. Phys. B **147**, 385 (1979); **147**, 448 (1979).
- [5] L.J. Reinders, H. Rubinstein, and S. Yazaki, Phys. Rept. **127**, 1 (1985).
- [6] S. Narison, World Sci. Lect. Notes Phys. **26**, 1 (1989); Nucl. Phys. B (Proc. Suppl.) **164**, 225 (2007); **207**, 315 (2010).
- [7] P. Colangelo and A. Khodjamirian, arXiv:hep-ph/0010175.
- [8] A.E. Dorokhov and W. Broniowski, Eur. Phys. J. C **32**, 79 (2003); Phys. Rev. D **78**, 073011 (2008); A.E. Dorokhov, *ibid.* **70**, 094011 (2004).
- [9] A.E. Dorokhov, Acta Phys. Polon. B **36**, 3751 (2005); Nucl. Phys. A **790**, 481 (2007); arXiv:hep-ph/0601114.
- [10] R. Barate *et al.* [ALEPH Collaboration], Z. Phys. C **76**, 15 (1997); Eur. Phys. J. C **4**, 409 (1998); S. Schael *et al.* [ALEPH Collaboration], Phys. Rept. **421**, 191 (2005).
- [11] M. Davier, A. Hocker, and Z. Zhang, Rev. Mod. Phys. **78**, 1043 (2006); M. Davier, S. Descotes-Genon, A. Hocker, B. Malaescu, and Z. Zhang, Eur. Phys. J. C **56**, 305 (2008).
- [12] K. Ackerstaff *et al.* [OPAL Collaboration], Eur. Phys. J. C **7**, 571 (1999).
- [13] D. Boito *et al.*, Phys. Rev. D **85**, 093015 (2012).
- [14] R.P. Feynman, *Photon-hadron interactions*, Reading, MA: Benjamin (1972) 282p.
- [15] A.V. Nesterenko and J. Papavassiliou, Phys. Rev. D **71**, 016009 (2005).
- [16] A.V. Nesterenko and J. Papavassiliou, J. Phys. G **32**, 1025 (2006).
- [17] A.V. Nesterenko, in Proc. of 9th Workshop on Nonperturbative QCD (Paris, France, 2007); eConf C0706044, 25 (2007); arXiv:0710.5878 [hep-ph].
- [18] F.J. Gilman, SLAC-PUB-1650 (1975).
- [19] S.L. Adler, Phys. Rev. D **10**, 3714 (1974).
- [20] A.V. Radyushkin, preprint JINR E2-82-159 (1982); JINR Rapid Commun. **78**, 96 (1996); arXiv:hep-ph/9907228.
- [21] N.V. Krasnikov and A.A. Pivovarov, Phys. Lett. B **116**, 168 (1982).
- [22] A.V. Nesterenko, in Proc. of 10th International Conference on Quark Confinement and the Hadron Spectrum (Munich, Germany, 2012); PoS (Confinement X), 350 (2013).
- [23] B. Schrempp and F. Schrempp, Z. Phys. C **6**, 7 (1980).
- [24] J.D. Bjorken, SLAC-PUB-5103 (1989).
- [25] A.L. Kataev and V.V. Starshenko, Mod. Phys. Lett. A **10**, 235 (1995).
- [26] G.M. Prosperi, M. Raciti, and C. Simolo, Prog. Part. Nucl. Phys. **58**, 387 (2007).
- [27] M.R. Pennington and G.G. Ross, Phys. Lett. B **102**, 167 (1981); M.R. Pennington, R.G. Roberts, and G.G. Ross, Nucl. Phys. B **242**, 69 (1984).
- [28] A.V. Nesterenko, Nucl. Phys. B (Proc. Suppl.) **186**, 207 (2009).
- [29] A.V. Nesterenko, in Proc. of 11th Workshop on Nonperturbative QCD (Paris, France, 2011); eConf C1106064, 23 (2011); arXiv:1106.4006 [hep-ph].
- [30] A.V. Nesterenko, Nucl. Phys. B (Proc. Suppl.) **234**, 199 (2013); arXiv:1110.3415 [hep-ph].

- [31] A.V. Nesterenko, in Proc. of 12th Workshop on Nonperturbative QCD (Paris, France, 2013) (to be published).
- [32] A.V. Nesterenko, in preparation.
- [33] A.I. Akhiezer and V.B. Berestetsky, *Quantum electrodynamics*, Interscience, NY (1965) 868p.
- [34] A.V. Nesterenko and J. Papavassiliou, Int. J. Mod. Phys. A **20**, 4622 (2005); Nucl. Phys. B (Proc. Suppl.) **152**, 47 (2005); **164**, 304 (2007).
- [35] M. Baldicchi, A.V. Nesterenko, G.M. Prosperi, D.V. Shirkov, and C. Simolo, Phys. Rev. Lett. **99**, 242001 (2007); M. Baldicchi, A.V. Nesterenko, G.M. Prosperi, and C. Simolo, Phys. Rev. D **77**, 034013 (2008).
- [36] A.V. Nesterenko, Phys. Rev. D **62**, 094028 (2000); **64**, 116009 (2001).
- [37] A.V. Nesterenko, Int. J. Mod. Phys. A **18**, 5475 (2003); Nucl. Phys. B (Proc. Suppl.) **133**, 59 (2004).
- [38] A.V. Nesterenko and C. Simolo, Comput. Phys. Commun. **181**, 1769 (2010); **182**, 2303 (2011); A.P. Bakulev and V.L. Khandramai, *ibid.* **184**, 183 (2013).
- [39] D.V. Shirkov and I.L. Solovtsov, Phys. Rev. Lett. **79**, 1209 (1997); Theor. Math. Phys. **150**, 132 (2007); K.A. Milton and I.L. Solovtsov, Phys. Rev. D **55**, 5295 (1997); **59**, 107701 (1999).
- [40] G. Cvetič and C. Valenzuela, Braz. J. Phys. **38**, 371 (2008); A.P. Bakulev, Phys. Part. Nucl. **40**, 715 (2009); N.G. Stefanis, *ibid.* **44**, 494 (2013); G. Cvetič and A.V. Kotikov, J. Phys. G **39**, 065005 (2012).
- [41] G. Cvetič, A.Y. Illarionov, B.A. Kniehl, and A.V. Kotikov, Phys. Lett. B **679**, 350 (2009); A.V. Kotikov, arXiv:1212.3733 [hep-ph].
- [42] M. Baldicchi and G.M. Prosperi, Phys. Rev. D **66**, 074008 (2002); AIP Conf. Proc. **756**, 152 (2005); M. Baldicchi, G.M. Prosperi, and C. Simolo, *ibid.* **892**, 340 (2007).
- [43] K.A. Milton, I.L. Solovtsov, and O.P. Solovtsova, Phys. Lett. B **439**, 421 (1998); Phys. Rev. D **60**, 016001 (1999); R.S. Pasechnik, D.V. Shirkov, and O.V. Teryaev, *ibid.* **78**, 071902 (2008).
- [44] N.G. Stefanis, Nucl. Phys. B (Proc. Suppl.) **152**, 245 (2006); A.P. Bakulev, K. Passek-Kumericki, W. Schroers, and N.G. Stefanis, Phys. Rev. D **70**, 033014 (2004); **70**, 079906(E) (2004); A.P. Bakulev, A.V. Pimikov, and N.G. Stefanis, *ibid.* **79**, 093010 (2009).
- [45] A.C. Aguilar, A.V. Nesterenko, and J. Papavassiliou, J. Phys. G **31**, 997 (2005); Nucl. Phys. B (Proc. Suppl.) **164**, 300 (2007).
- [46] J. Beringer *et al.* [Particle Data Group Collaboration], Phys. Rev. D **86**, 010001 (2012).
- [47] W.J. Marciano and A. Sirlin, Phys. Rev. Lett. **56**, 22 (1986); **61**, 1815 (1988); E. Braaten and C.S. Li, Phys. Rev. D **42**, 3888 (1990).
- [48] E. Braaten, S. Narison, and A. Pich, Nucl. Phys. B **373**, 581 (1992).
- [49] P.A. Baikov, K.G. Chetyrkin, and J.H. Kuhn, Phys. Rev. Lett. **101**, 012002 (2008); **104**, 132004 (2010).
- [50] P.A. Baikov, K.G. Chetyrkin, J.H. Kuhn, and J. Rittinger, Phys. Lett. B **714**, 62 (2012).
- [51] K.A. Milton, I.L. Solovtsov, and O.P. Solovtsova, Phys. Rev. D **64**, 016005 (2001); Mod. Phys. Lett. A **21**, 1355 (2006).
- [52] G. Cvetič and C. Valenzuela, Phys. Rev. D **74**, 114030 (2006); **84**, 019902(E) (2011); C. Ayala, C. Contreras, and G. Cvetič, *ibid.* **85**, 114043 (2012).